Ortiz Serna, MP.; Díaz Calleja, R.; Sanchis Sánchez, MJ.; Riande, E.; Numes, R.; Martins, A.; Visconte, L. (2011). Dielectric spectroscopy of natural rubber-cellulose II nanocomposites. Journal of Non-Crystalline Solids. 357(2):598-604. doi:10.1016/j.jnoncrysol.2010.06.044

Dielectric Spectroscopy of the dynamics in Natural Rubber-Cellulose II nanocomposites

P. Ortiz-Serna[a,*], R. Díaz-Calleja[a], M. J. Sanchis[a], E. Riande[b], R. Nunes[c], A. Martins[c], L. Visconte[c]

[a]*Departamento de Termodinámica Aplicada, E.T.S.I.I., Instituto de Tecnología Eléctrica Universitat Politècnica de Valencia, Camino de Vera s/n, 46022 Valencia, Spain*

[b]*Instituto de Ciencia y Tecnología de Polímeros (CSIC), 28006 Madrid, Spain*

[c]*Instituto de Macromoleculas Professora Eloisa Mano, Universidade Federal do Rio de Janeiro, P.O. Box 68525, Brazil*

**Corresponding author. e-mail: portiz@ter.upv.es*

Abstract

Nanocomposite materials obtained from natural rubber (NR) reinforced with different amounts of cellulose II nanoparticles (in the range of 0 to 30 phr) are studied by dielectric spectroscopy (DS) in the high temperature range (50 to 150 ºC). The obtained spectra exhibit conductivity phenomena at low frequencies and high temperatures. The samples were also studied in the dry state. For comparative purpose the pure materials, NR and cellulose, are also investigated. An explanation is given concerning the cellulose effect on the conductive properties of the dry and wet nanocomposites.

KEYWORDS. Dielectric spectroscopy, natural rubber, cellulose II, nanocomposites, conductivity.

1. Introduction

Dielectric spectroscopy suffers a central problem, which is fundamental for all types of spectroscopic methods, that is to assign empirically separated processes to corresponding molecular processes. For solid biopolymers like NR and cellulose, having various complex structural levels with different length scales and different response times, this task is very complicated, and therefore it is controversial in the literature.

The dielectric response of a material at high temperatures and low frequencies is often dominated by conduction effects. The processes that contribute to the dielectric response under these conditions include the migration of mobile charge carriers across the medium and the trapping of charges at interfaces and boundaries. While the motion of charge carriers can increase the dielectric loss by several orders of magnitude, charge trapping influences both, the dielectric constant and the dielectric loss. This additional polarization is the result of (i) accumulation of charges at the electrode-sample interface, called "electrode polarization" (EP) [1] and/or (ii) the separation of charges at internal phase boundaries referred to as Maxwell-Wagner-Sillars (MWS) polarization [2,3]. MWS polarization is generally evident in non-homogenous materials like multiphase polymers, blends and colloids, crystalline or liquid crystalline polymers, etc. and occurs across smaller size scales as compared to electrode polarization. The MWS effects are more pronounced for conductive materials and, in certain cases, this large scale polarization can mask the dielectric orientation response of the material.

In our firsts papers [4,5] we discussed the molecular origin of the dielectric relaxation processes found in the nanocomposites series and in pure materials at low temperatures. These spectra exhibit: (a) two overlapped α-relaxations associated respectively with the dynamic glass transitions of NR (faster process) and of the lipid present in the NR; (b) a β-relaxation associated with local chain dynamics of cellulose and (c) a relaxation process

associated to the water present in the samples. In the high temperature range (50 to 150 ºC), both conductive processes above described (MWS and EP) are found in the analyzed nanocomposites.

In order to characterize the conductive processes it is advisable to represent the obtained dielectric data in terms of the conductivity magnitude $\sigma^*(\omega)$. According to Maxwell's equations [6] the current density $j = \sigma^* E$ and the time derivative of the dielectric displacement $\frac{dD}{dt} = i\omega\varepsilon^*\varepsilon_0 E$ are equivalent, where $\sigma^*(\omega)$ is the complex conductivity. Hence, for sinusoidal electrical fields $E(\omega) = E_0 e^{i\omega t}$ and $\varepsilon^*(\omega)$ and $\sigma^*(\omega)$ are related to each other by

$$\sigma^*(\omega) = \sigma'(\omega) + i\,\sigma''(\omega) = i\,\omega\,\varepsilon_0\,\varepsilon^*(\omega)$$

The real and imaginary part of $\sigma^*(\omega)$ are given by

$$\sigma'(\omega) = \omega\,\varepsilon_0\,\varepsilon''(\omega); \qquad \sigma''(\omega) = \omega\,\varepsilon_0\,\varepsilon'(\omega)$$

The topic of the present paper is the analysis or, more properly, the phenomenological description and the molecular interpretation of these high temperature relaxation processes found in the solid state, as well as the effect of the cellulose nanoparticles and water in the nanocomposites conductivity behaviour.

2. Experimental

2.1. Samples

The nanocomposites series consist in four samples: NR 10, NR 15, NR 20, and NR 30 in which the content of cellulose II vary from 10 to 30 phr respectively. The syntheses of the nanocomposites were carried out in the Instituto de Macromoléculas Professora Eloisa Mano (Universidade Federal do Rio de Janeiro) [7]. These materials were processed to obtain sheets with thickness of around 0.25 mm.

2.2. Dielectric Spectroscopy (DS)

DS [1, 8-10] experiments were performed in a Broadband Dielectric Spectrometer System, based on an Alpha analyzer and a Quatro temperature controller. Isothermal measurements were carried out at 44 frequencies between $5 \cdot 10^{-2}$ and $3 \cdot 10^{6}$ Hz from 50 to 150 ºC, in 5 ºC steps, using gold electrodes of 20 mm of diameter. The accuracy of Alpha impedance measurement is 0.01 %. The dielectric measurements were carried out in the samples as received and also in the dried samples. The latter were obtained via drying in an air-circulating oven at 70 ºC until constant weight.

3. Results

3.1. DS

The thermal measurements (Differential Scanning Calorimetry) of the samples [4,5] revealed the presence of some moisture in the as received samples (called "wet" below). In order to elucidate the influence of the presence of water, dielectric measurements were carried out in both wet and dry samples.

Figure 1 gives the complex conductivity representation for the experimental data. For the real part (σ') on the low frequency side a plateau is observed for the highest temperatures. This plateau represents the dc-conductivity of the sample, which increases with growing temperature and is clearly marked only for the highest temperatures. From the obtained plateau, the d.c.-conductivity value, σ_{DC}, can be extrapolated for $\omega \to 0$.

Besides, as explained above, differences in conductivity of the phases of an inhomogeneous medium, give rise to interfacial polarization, the built-up of space charges near the interfaces between the various phases (MWS-relaxation). Such a polarization usually occurs at frequencies lower than the time scales typical of dipolar polarizations.

In the middle part of the isotherm the MWS-relaxation creates a ‘knee’-like increase of the σ-curve which is uniformly shifted with the temperature. At lower temperatures this ‘wriggle’ is in the range of the σ_{DC}-plateau, which makes it impossible to determine directly the dc-conductivity.

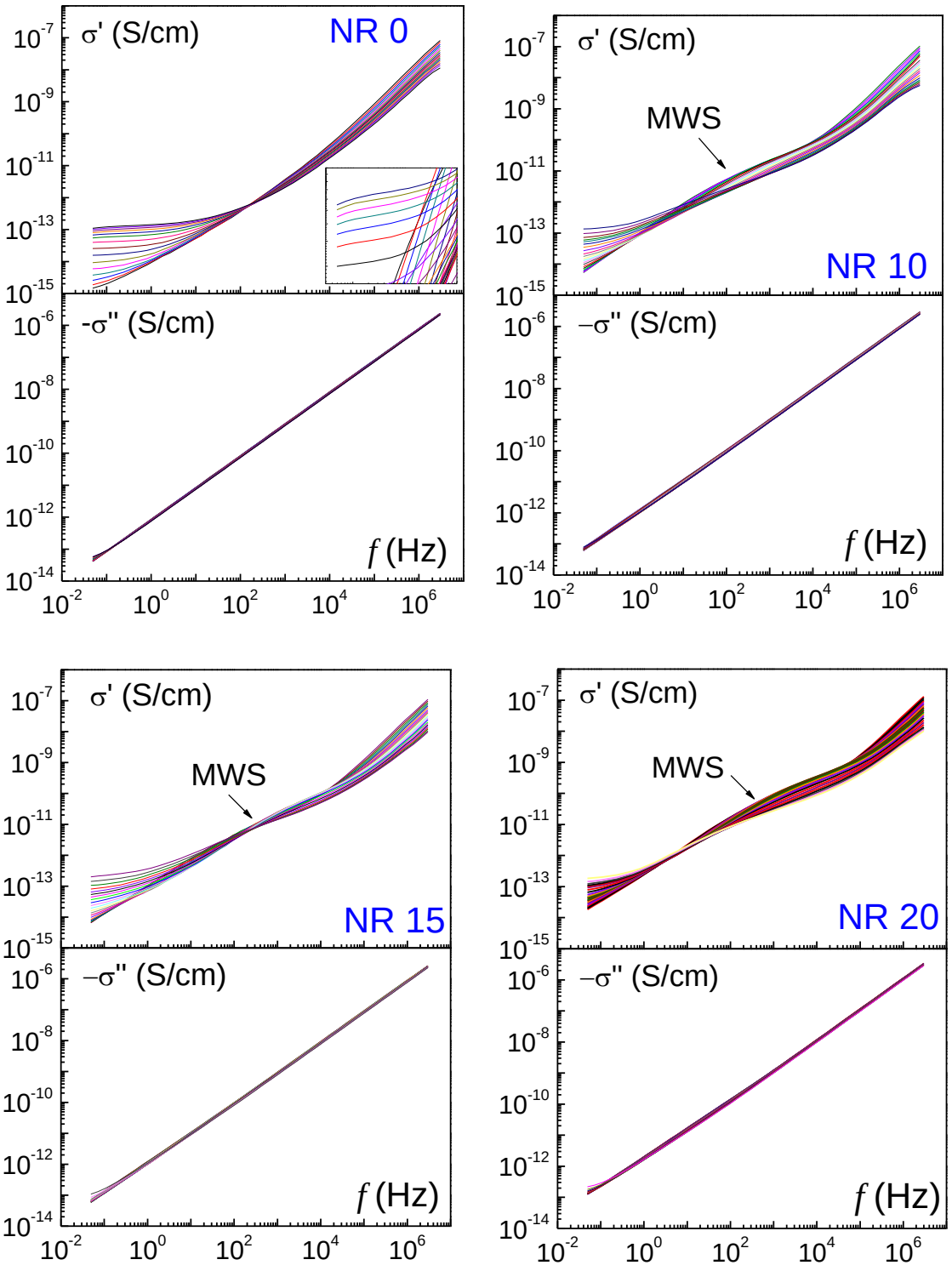

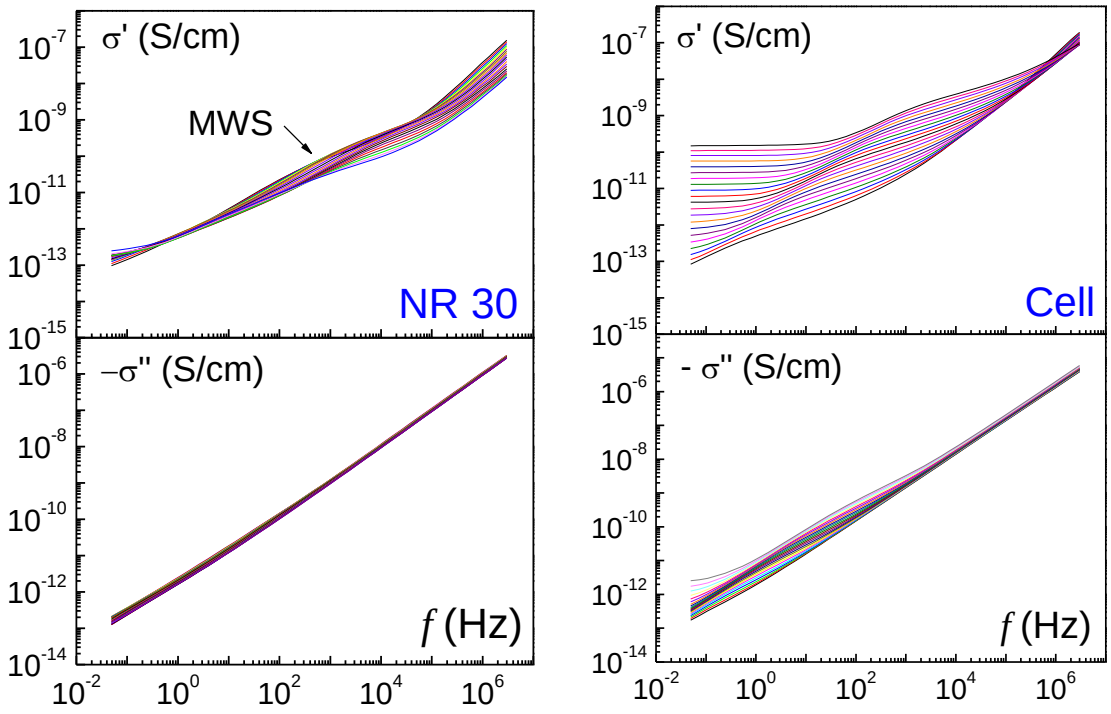

Figure 1. *Frequency dependence of the complex conductivity at several temperatures for the wet nanocomposites.*

The MWS polarization takes place in all the compositions (**Figure 2**) and the process intensity rises with the cellulose content since the internal interfaces also rise. The major effect of even low contents of water in the samples is the increase of the electrical conductivity of the sample, which superposes the dielectric processes in the loss spectra [5]. Therefore, the dc conductivity (σ_{DC}) must be simultaneously determined from the conductivity spectra (log σ' versus *f*). The frequency dependence of the conductivity is also masked by the dielectric relaxation effects and by the electrode polarization (leading to a Debye-like relaxation) in the very low frequency range, as it is observed in **Figure 1**. The plateau observed at the highest temperatures in all the compositions was not enough clearly to calculate σ_{DC} values by extrapolation.

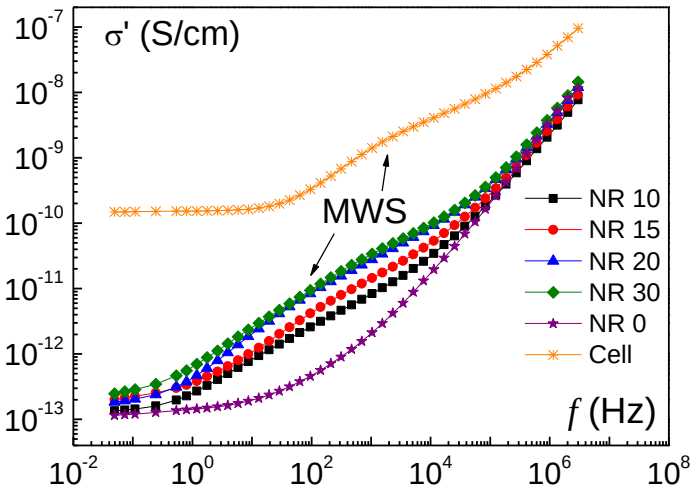

Figure 2 *Real part of the complex conductivity, σ^*, as a function of frequency for wet NR and nanocomposites at 150 ºC.*

The imaginary part of the complex conductivity decreases with decreasing frequency. The increase observed at low frequencies indicates the presence of the electrode polarization phenomenon (**Figure 3**).

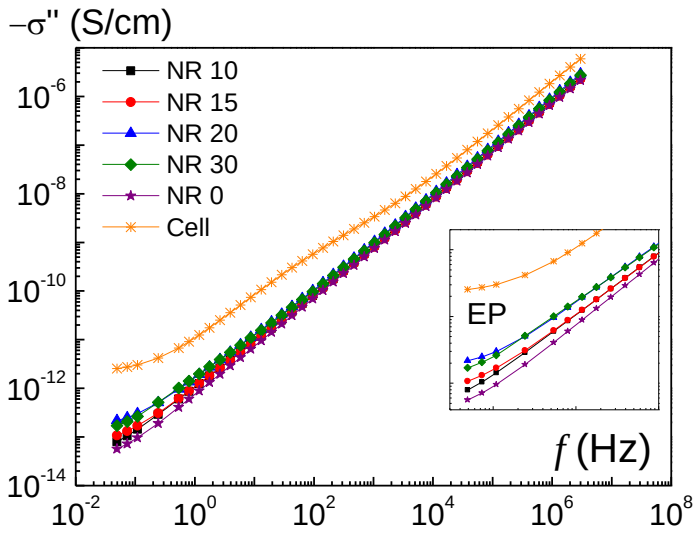

Figure 3 *Imaginary part of the complex conductivity, σ^*, as a function of frequency for wet NR and nanocomposites at 150 ºC.*

Results obtained for the dry nanocomposites are shown in **Figure 4** as the frequency dependence of the real (σ') and imaginary (σ'') part of the conductivity at several temperatures. For the real part (σ') on the low frequency side a plateau is observed for the highest temperatures. This plateau represents the dc-conductivity of the sample, which increases with growing temperature and is clearly marked for the highest temperatures.

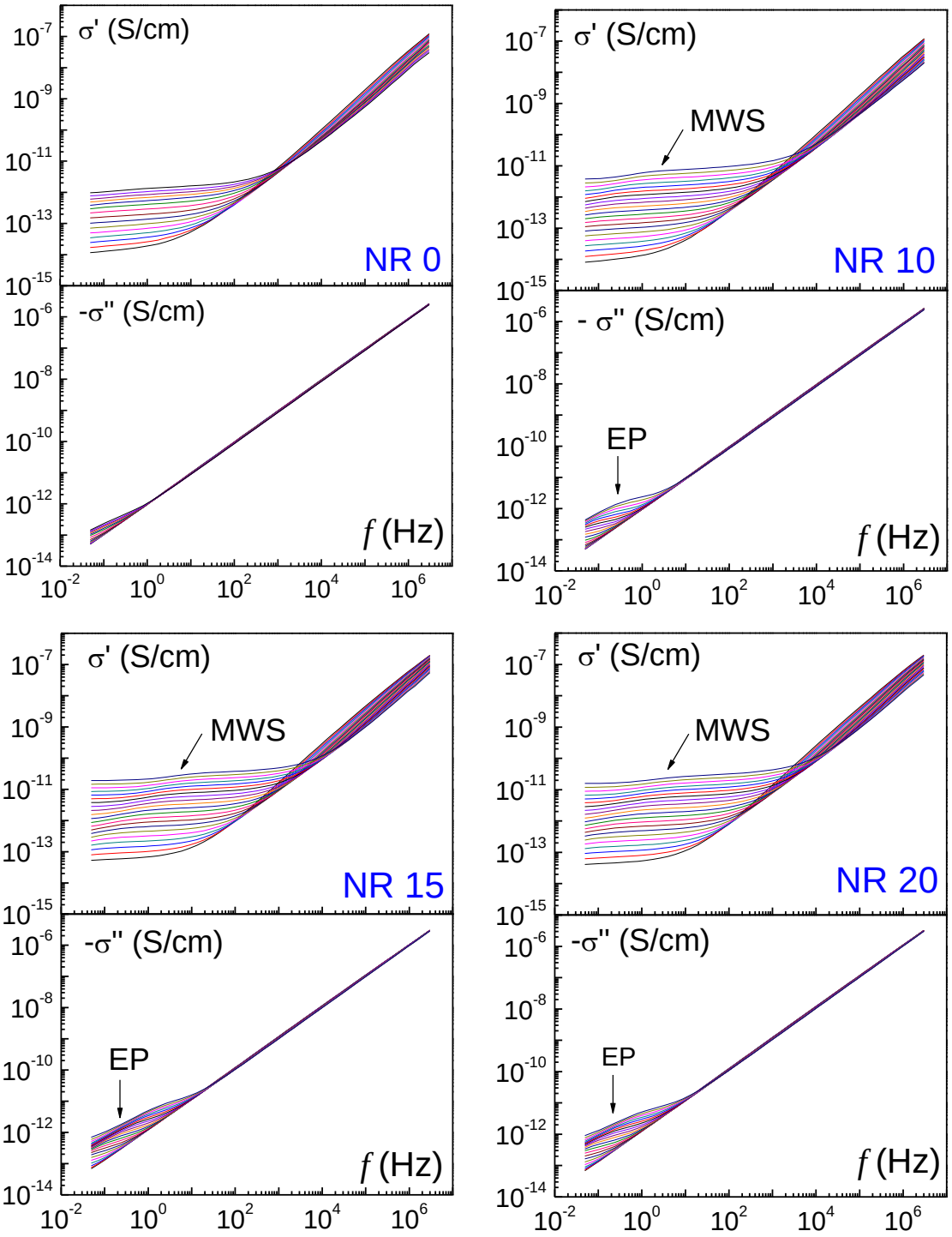

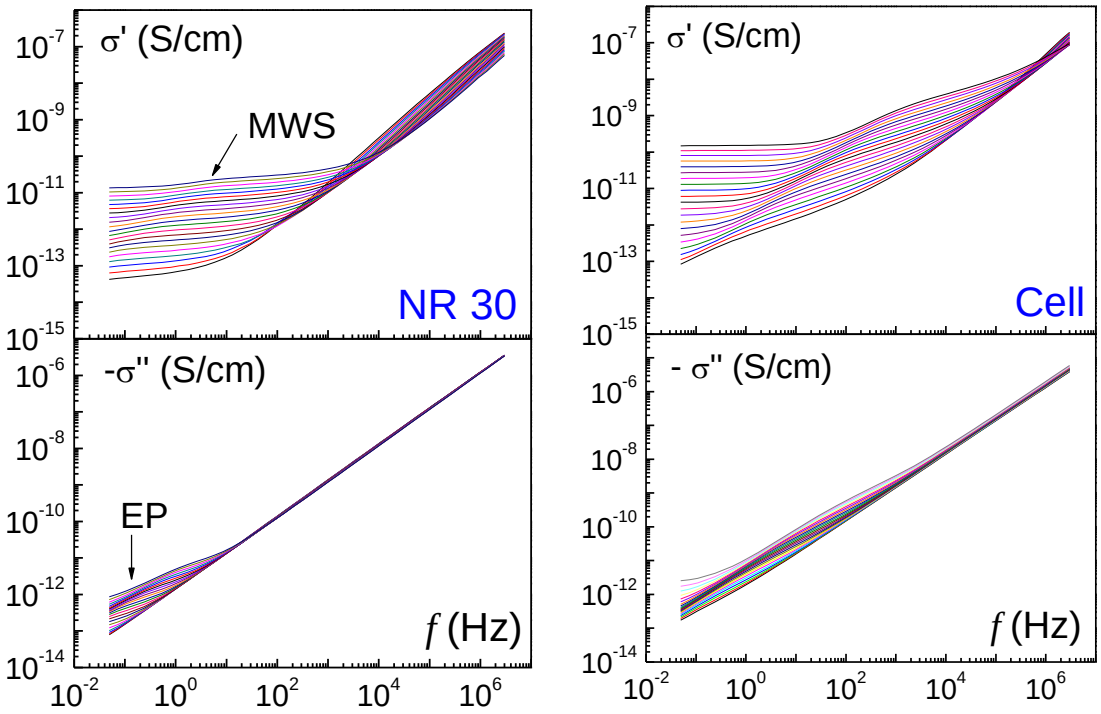

Figure 4 *Frequency dependence of the real and imaginary part of dielectric conductivity at several temperatures (from -130 to 150 ºC) for the dry nanocomposites.*

From the σ' representations in **Figure 4**, σ_{DC} values were determined from the plateau at low frequencies side ($\sigma \rightarrow 0$). Temperature dependence of the σ_{DC} values calculated for all the nanocomposites has a linear (Arrhenius) character. Arrhenius plots for the nanocomposites are presented in **Figure 5**. Activation energies and σ_0 values obtained from the corresponding fits (equation 1) are summarized in **Table 1**. Values of the activation energy for the σ-process are similar for all the samples and lies between 72-75 kJ/mol.

$$\sigma_{DC} = \sigma_0 \exp\left(\frac{-E_a}{RT}\right) \qquad (1)$$

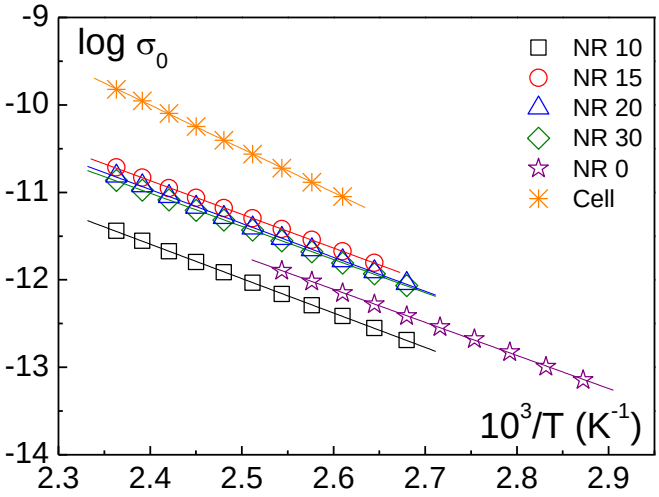

Figure 5 *Activation plot of the dc-conductivity for dry NR 0 and nanocomposites. The dashed lines are the fits to the AR equation.*

Table 1. *AR fit parameters for the σ-relaxation process in dry NR and nanocomposites*

σ-relaxation	log σ_0	E_a (kJ/mol)
Cell	-2.01 ± 0.05	95.8 ± 0.4
NR 0	-2.27 ± 0.06	72.4 ± 0.4
NR 10	-2.14 ± 0.04	75.4 ± 0.3
NR 15	-1.62 ± 0.04	73.8 ± 0.3
NR 20	-1.66 ± 0.06	74.2 ± 0.5
NR 30	-1.92 ± 0.03	72.6 ± 0.2

As in the wet samples, differences in conductivity of the phases of an inhomogeneous medium, give rise to interfacial polarization (MWS-relaxation); creating a 'knee'-like increase in the σ-curve. The MWS polarization takes place in all the compositions (**Figure 6**) and the process intensity is very similar for NR 15, 20 and 30 samples. The imaginary part of the complex conductivity decreases with decreasing frequency. The increase at low frequencies again indicates the existence of the electrode polarization process (**Figure 7**).

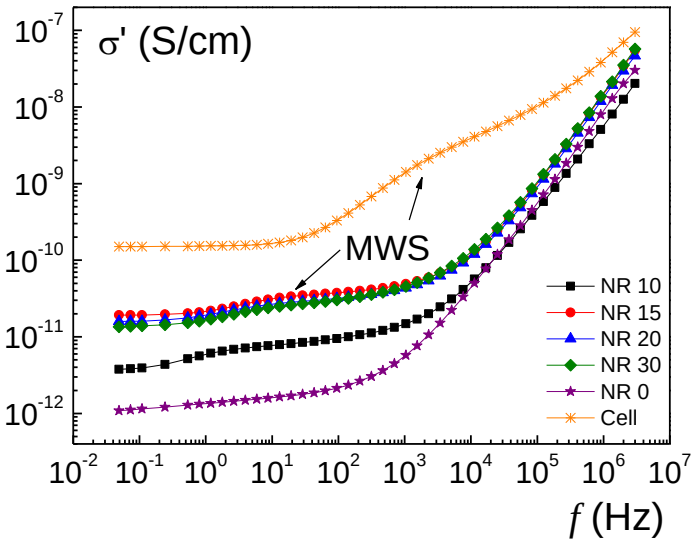

Figure 6 *Frequency dependence of the dielectric conductivity real part at 150 ºC for the dry NR and nanocomposites.*

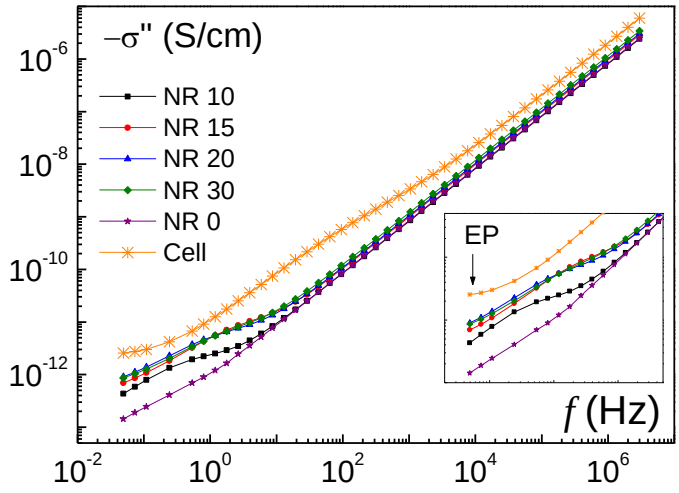

Figure 7 *Frequency dependence of the dielectric conductivity imaginary part at 150 ºC for the dry NR and nanocomposites.*

In order to study the moisture effect on the temperature dependence of σ^*, in **Figures 8** and **9** are represented a comparison of σ' and σ'' for the wet and dry samples. It is observed that MWS process is better defined and more intense in the dry samples than in the wet ones (**Figure 8**). This difference can be explained by the changes in the internal interfaces that take place with the water elimination. In accordance with our results, the water

elimination would favour the polarization process in the interfaces that exist between the different components of our heterogeneous systems.

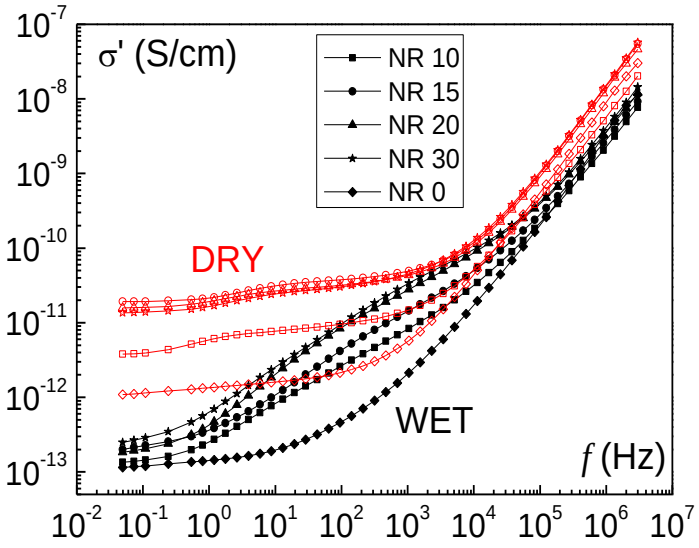

Figure 8 *Comparison of the dielectric conductivity real part at 150 ºC for the dry (open symbols) and wet (full symbols) NR and nanocomposites.*

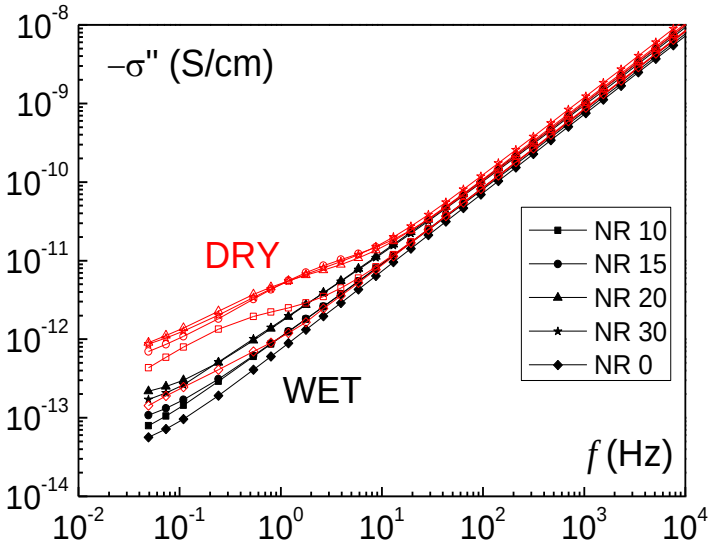

Figure 9 *Comparison of the dielectric conductivity imaginary part at 150 ºC for the dry (open symbols) and wet (full symbols) NR and nanocomposites.*

5. Conclusions

Wet nanocomposites present higher conductivity than NR 0, and become more conductive as the cellulose content rises due to the water and polar groups increase in the samples. Also the intensity of MWS polarization increases with the cellulose content because

of the rise of internal interfaces. In this case, the d.c.-conductivity values, σ_{DC}, could not be extrapolated from σ' plot at $\omega \to 0$ because the plateau observed at the highest temperatures was not enough clearly.

As well as for the wet samples, MWS and EP processes are observed in the dry nanocomposites. Nanocomposites present higher conductivity than NR 0, and NR 15, 20 and 30 samples show more or less the same conductivity. Also the intensity of MWS polarization is very similar in these samples. For dry nanocomposites, the d.c.-conductivity values, σ_{DC}, were calculated to obtain an average value of 74 kJ/mol.

Acknowledgements

This work was financially supported by the DGCYT through Grant MAT2008-06725-C03.

References

[1] Kremer, F.; Schönhals, A. *Broadband Dielectric Spectroscopy*, (Eds) Springer-Verlag Berlin Heidelberg New York, 2003.

[2] Wagner, K. W.; *Arch Electrotech* **1914**, *2*, 371.

[3] Sillars, R. W.; *Inst Elect Eng* **1937**, *80*, 378.

[4] Ortiz-Serna, P.; Díaz-Calleja, R.; Sanchis, M. J.; Floudas, G.; Nunes, R.; Macromolecules **2010**, *43*, 5094–5102.

[5] Ortiz-Serna, P.; Díaz-Calleja, R.; Sanchis, M. J.; Riande, E.; Nunes, R.; Journal of Non-Crystalline Solids **2011**, *357*, 598–5604.

[6] Maxwell, J. C.; *Phil Trans* **1865**, *155*, 459.

[7] Martins, A. F.; Visconte, L. L. Y.; Nunes, R. C. R. *Kautschuk Gummi Kunststoffe* **2002**, *55 (12)*, 637-641.

[8] McCrum, N.G.; Read, B.E; Williams, W. *Anelastic and Dielectric Effects in Polymeric Solids*, Dover Publications, Inc., New York, 1991, 118.

[9] Riande, E.; Díaz Calleja, R. *Electrical Properties of Polymers*, Marcel Dekker Inc., 2004.

[10] Jonscher, A. K. *Dielectric Relaxation in Solids*, Chelsea Dielectric press., 1983.

Figure captions

Figure 1. Frequency dependence of the complex conductivity at several temperatures for the wet nanocomposites.

Figure 2. Real part of the complex conductivity, σ^*, as a function of frequency for wet NR and nanocomposites at 150 ºC.

Figure 3. Imaginary part of the complex conductivity, σ^*, as a function of frequency for wet NR and nanocomposites at 150 ºC.

Figure 4. Frequency dependence of the real and imaginary part of dielectric conductivity at several temperatures (from -130 to 150 ºC) for the dry nanocomposites.

Figure 5. Activation plot of the dc-conductivity for dry NR 0 and nanocomposites. The dashed lines are the fits to the AR equation.

Figure 6. Frequency dependence of the dielectric conductivity real part at 150 ºC for the dry NR and nanocomposites.

Figure 7. Frequency dependence of the dielectric conductivity imaginary part at 150 ºC for the dry NR and nanocomposites.

Figure 8. Comparison of the dielectric conductivity real part at 150 ºC for the dry (open symbols) and wet (full symbols) NR and nanocomposites.

Figure 9. Comparison of the dielectric conductivity imaginary part at 150 ºC for the dry (open symbols) and wet (full symbols) NR and nanocomposites.